17 August 2011

ESI for:

The oxidative conversion of the *N,S*-bridged complexes [{RhLL'(μ-X)}$_2$] to [(RhLL')$_3$(μ-X)$_2$]$^+$ (X = mt or taz): a comparison with the oxidation of *N,N*-bridged analogues

Robin J. Blagg, María J. López-Gómez, Jonathan P.H. Charmant, Neil G. Connelly *, John J. Cowell, Mairi F. Haddow, Alex Hamilton, A. Guy Orpen, Thomas Riis-Johannessen and Saowanit Saithong.

Table S1 ^{13}C-{^{1}H} NMR spectroscopic data [a] for [{RhLL'(μ-taz)}$_2$].

Complex	
[{Rh(cod)(μ-taz)}$_2$] **2**	162.04 (s, taz *C*^{5}), 149.97 (s, taz *C*^{3}), 79.35 (br s, cod *C*H), 39.84 (s, taz 4-*C*H$_2$CH$_2$), 31.71 (br s, cod *C*H$_2$), 14.86 (s, taz 3-*C*H$_3$), 11.28 (s, taz 4-C$_2$*C*H$_3$)
[{Rh(CO)$_2$(μ-taz)}$_2$] **4**	187.64 (d, $^1J_{CRh}$ 64.5, *C*O)†, 186.14 (d, $^1J_{CRh}$ 66.2, *C*O)‡, 185.05 (d, $^1J_{CRh}$ 68.0, *C*O)‡, 182.86 (d, $^1J_{CRh}$ 69.1, *C*O)†, 162.83 (d, $^2J_{CRh}$ 2.9, taz *C*^{5})‡, 162.33 (br s, taz *C*^{5})†, 151.20 (s, taz *C*^{3})‡, 150.62 (s, taz *C*^{3})†, 40.17 (s, taz 4-*C*H$_2$CH$_3$)†‡, 14.58 (s, taz 3-*C*H$_3$)‡, 14.52 (s, taz 3-*C*H$_3$)†, 11.50 (s, taz 4-CH$_2$*C*H$_3$)‡, 11.20 (s, taz 4-CH$_2$*C*H$_3$)† [b]
[{Rh(CO)(PPh$_3$)(μ-taz)}$_2$] **6**	162.50 (s, taz *C*^{5}), 148.77 (s, taz *C*^{3}), 135.10 (d, J_{CP} 13.1, P*Ph*$_3$), 134.74 (d, J_{CP} 45.4, P*Ph*$_3$), 130.16 (s, P*Ph*$_3$), 128.07 (d, J_{CP} 10.0, P*Ph*$_3$), 39.23 (s, taz 4-*C*H$_2$CH$_3$), 14.83 (s, taz 3-*C*H$_3$), 10.91 (s, taz 4-CH$_2$*C*H$_3$)
[{Rh[P(OPh)$_3$]$_2$(μ-taz)}$_2$] **7**	152.61 {d, J_{CP} 59.2, P(O*Ph*)$_3$}, 152.56 {d, J_{CP} 60.7, P(O*Ph*)$_3$}, 129.41 {d, J_{CP} 43.1, P(O*Ph*)$_3$}, 123.79 {d, J_{CP} 39.2, P(O*Ph*)$_3$}, 121.84 {d, J_{CP} 6.92, P(O*Ph*)$_3$}, 40.14 (s, taz 4-*C*H$_2$CH$_2$), 15.00 (s, taz 3-*C*H$_3$), 11.38 (s, taz 4-CH$_2$*C*H$_3$)

[a] Chemical shift (δ) in ppm, *J* values in Hz, spectra in CD_2Cl_2 at 20 °C. [b] Two isomers present at a ratio of 3†:2‡.

Table S2 ^{13}C-{^{1}H} NMR spectroscopic data [a] for [{RhLL'}$_3$(μ-taz)$_2$]$^+$.

Complex	
[{Rh(cod)}$_3$(μ-taz)$_2$][PF$_6$] **9**$^+$[PF$_6$]$^-$	155.48 (br s, taz *C*^{5}), 153.40 (s, taz *C*^{3}), 91.20 (d, $^1J_{CRh}$ 13.2, cod *C*H), 90.02 (d, $^1J_{CRh}$ 11.5, cod *C*H), 86.76 (d, $^1J_{CRh}$ 10.9, cod *C*H), 85.62 (d, $^1J_{CRh}$ 10.9, cod *C*H), 82.54 (d, $^1J_{CRh}$ 11.5, cod *C*H), 80.05 (d, $^1J_{CRh}$ 12.1, cod *C*H), 41.60 (s, taz 4-*C*H$_2$CH$_2$), 36.60 (s, cod *C*H$_2$), 35.15 (s, cod *C*H$_2$), 35.07 (s, cod *C*H$_2$), 29.30 (s, cod *C*H$_2$), 28.33 (s, cod *C*H$_2$), 28.24 (s, cod *C*H$_2$), 15.01 (s, taz 3-*C*H$_3$), 11.28 (s, taz 4-CH$_2$*C*H$_3$)
[{Rh(CO)$_2$}$_3$(μ-taz)$_2$][PF$_6$] **11**$^+$[PF$_6$]$^-$	183.98 (d, $^1J_{CRh}$ 68.0, *C*O), 183.84 (d, $^1J_{CRh}$ 68.0, *C*O), 180.66 (d, $^1J_{CRh}$ 68.0, *C*O), 163.08 (s, taz *C*^{5}), 158.20 (s, taz *C*^{3}), 42.12 (s, taz 4-*C*H$_2$CH$_2$), 14.76 (s, taz 3-*C*H$_3$), 11.93 (s, taz 4-CH$_2$*C*H$_3$)
[{Rh(CO)(PPh$_3$)}$_3$(μ-taz)$_2$][PF$_6$] **13**$^+$[PF$_6$]$^-$	152.94 (s, taz *C*^{3}), 152.42 (s, taz *C*^{3}), 135.4-128.6 (m, P*Ph*$_3$), 40.40 (s, taz 4-*C*H$_2$CH$_2$), 40.28 (s, taz 4-*C*H$_2$CH$_2$), 14.76 (s, taz 3-*C*H$_3$), 14.33 (s, taz 3-*C*H$_3$), 10.75 (s, taz 4-CH$_2$*C*H$_3$), 10.49 (s, taz 4-CH$_2$*C*H$_3$)

[a] Chemical shift (δ) in ppm, *J* values in Hz, spectra in CD_2Cl_2 at 20 °C.

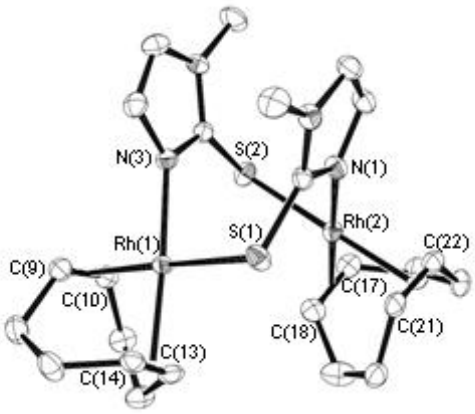

Figure S1 Molecular structure of [{Rh(cod)(μ-mt)}$_2$] **1**. (Ellipsoids are shown at the 50% probability level; hydrogen atoms are omitted for clarity.)

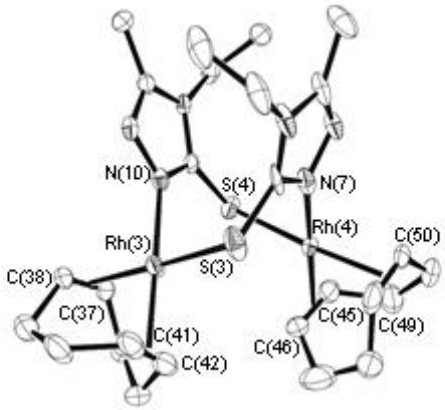

Figure S2 Molecular structure of [{Rh(cod)(μ-taz)}$_2$] **2** (The second of two inequivalent molecules in the unit cell.)

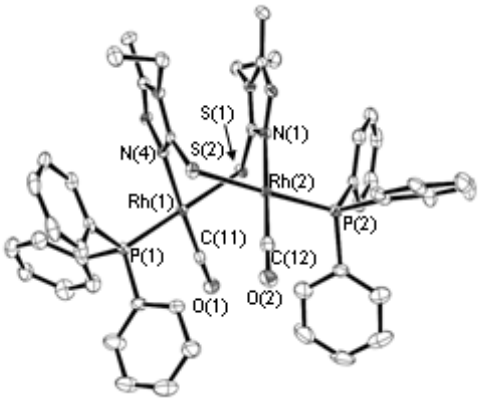

Figure S3 Molecular structure of [{Rh(CO)(PPh$_3$)(μ-taz)}$_2$] **6**.

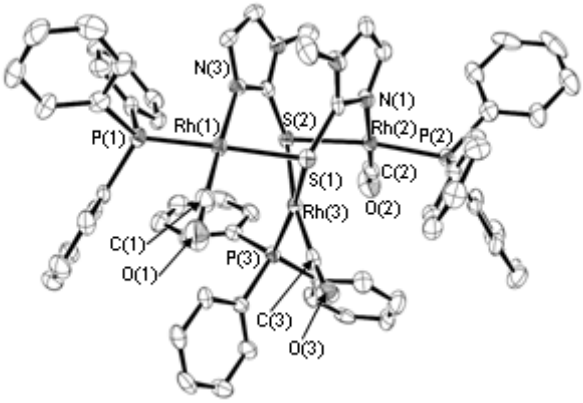

Figure S4 Structure of the cation [{Rh(CO)(PPh$_3$)}$_3$(μ-mt)$_2$]$^+$ **12**$^+$.